

Supplementary Information

Novel alligator cathelicidin As-CATH8 demonstrates anti-infective activity against clinically relevant and crocodylian bacterial pathogens

Felix L. Santana^{1,2}, Karel Estrada³, Morgan A. Alford², Bing C. Wu², Melanie Dostert², Lucas Pedraz², Noushin Akhoundsadegh², Pavneet Kalsi², Evan F. Haney², Suzana K. Straus⁴, Gerardo Corzo^{1,*}, and Robert E. W. Hancock^{2,*}

¹ Departamento de Medicina Molecular y Bioprocesos, Instituto de Biotecnología, Universidad Nacional Autónoma de México, Cuernavaca, 62210, Morelos, Mexico.

² Centre for Microbial Diseases and Immunity Research, University of British Columbia, Vancouver, V6T 1Z4, BC, Canada.

³ Unidad de Secuenciación Masiva y Bioinformática, Instituto de Biotecnología, Universidad Nacional Autónoma de México, Cuernavaca, 62210, Morelos, Mexico.

⁴ Department of Chemistry, University of British Columbia, Vancouver, V6T 1Z1, BC, Canada.

* Correspondence: gerardo.corzo@ibt.unam.mx (GC); bob@hancocklab.com (REWH)

Keywords: cathelicidins; antimicrobial peptides; LL-37; biofilms; abscess model; skin model; reptiles

Supplementary Tables

Table S1	Cathelicidin sequences identified in <i>Alligator mississippiensis</i> , <i>Alligator sinensis</i> , <i>Crocodylus porosus</i> , and <i>Gavialis gangeticus</i>	3
Table S2	Summary of prediction of identified cathelicidin sequences from <i>A. mississippiensis</i> , <i>A. sinensis</i> , <i>C. porosus</i> , and <i>G. gangeticus</i>	6
Table S3	Vertebrate cathelicidins peptides included in the phylogenetic analysis . .	7
Table S4	Antimicrobial activity of the crocodylian cathelicidins	8
Table S5	Biofilm inhibitory activity of the crocodylian cathelicidins	9

Supplementary Figures

Figure S1	Multiple sequence alignment of novel and previously identified crocodylian cathelicidins	10
Figure S2	Biofilm inhibitory activity of crocodylian cathelicidin peptides against different bacterial pathogens	11
Figure S3	Cytotoxic activity of crocodylian cathelicidins against human cells	12
Figure S4	Bacterial membrane depolarization and permeabilization capacity of As-CATH8	13
Figure S5	DNA binding activity of As-CATH8	14

Supplementary Tables

Table S1: Cathelicidin sequences identified in *Alligator mississippiensis*, *Alligator sinensis*, *Crocodylus porosus* and *Gavialis gangeticus*. Previously described alligator cathelicidins AM-36 [1] (renamed here as Am-CATH4) and As-CATH1-6 [2] were also recovered in our analysis and are included as a reference. Putative elastase cleavage site that indicates the start of the mature sequence is denoted with an arrow (↓) and was inferred based on protein sequence alignment with As-CATH1-6 [2]. NCBI accession numbers and references are shown.

Name	Sequence	Accession
Am-CATH1	MGRWGWGVLLGLAMLVASASASQHKMLSYYEAVSLAVDFYNQEPGIDHAFRLRLRA DPQPAWDMTSKPRQELQFVVRETVCRAQDPPASECDFKDNGLVRNCTGLFSMER ESPTVIITCDTVPTEQHVRV↓TRSERRNGHKRRRGSGSRRGQYSSTKHGGRKHP RKRPGSGSRLGHETPHVAPIDKGHV	OL889930
Am-CATH3	MGCRGWGVLLGLATLVAAASASQRKMLTYREAAFAVDFYNRQPGIDHTFQLLSV EPQVPDTSKSRQEVRFVVCETVCPQADNHPDSECNIFNGLVRNCMWLLSTEH KLPTSIITCDTVPKGHV↓PANPKLPGKGPGRHPSSGIWRGQGTFFSLPITKK PVG	OL889932
Am-CATH4	PDRV↓RRGLFKKLRRKIKKGFKKIFKRLPPIGVGVSIPLAGKR	Barksdale et al., OL889933
Am-CATH5	METCLCLLLLLGVATAVATAQAQAQTSQSQAQYEDAVTTAVDIFNQESGLPQ AYRLLEAEPQSEWNPSSQAAQPLKFSVKETVCPIAQKGNLKCDFKENGVLVKDCS GLFTAGKKPPVTAVKCEDTSQEPELV↓TRRKFWKILNGALKIAPFFLG	OL889934
Am-CATH6	MKSCWALVLLVGCMASAATAQSQNLNFNEAVSLAVDFYNRGLAVNNTFQLLRAPS GDVSSPSEFRRLNFTIMETTCVGSQPTQELCQFKENGLVRACVGFSTQQVAP LIVVTCEEAPSEPV↓RVTRWLWLLRGGLKAAGWGIRAHNLNRN	OL889935
Am-CATH8	APPAPALSSYQEALAAAVNTYNQESGLPQAYRLLEAEPQWPSSQPAQPLKFS IKETECLVSEKRDVSQCPFKDKGLVKDCKGLYAEKEPPVITAKCEDAGQEPQLV ↓KRVNWPVKVGRVLRFLPYILGG	OL889936
Am-CATH11	MLVASASASQHKMLSYYEAVSLAVDFYNQEPGIDHAFRLRLRADPQPAWDMTSKPR QELQFVVRETVCRAQDPPASECDFKDNGLVRNCTGLFSMERESPTVIITCDTVP TEQHVRV↓RRSGWNNRSKRRRGSGSRRGRFSHIAHGGRKGHERIARV	OL889931

As-CATH1	MGRWGWGVLLGLAMLVASASASQHKTLSYEEAVSLAVDFYNQEPGIDHAFRLRLRA DPQPAWDMTSKPRQELRFVVRETVCRAQDPPASECDFKDNLVRNCTGLFSTER ESPTVIITCDTVPQGHRV↓RRSGWWNGHKRRRGSGSRHGQYSSTKYGGRKRP RKRPGSGSWLSHDTPHVAPIAKGHVG	Chen et al., ASN73761
As-CATH2	MGRWGWGVLLGLATFVAVALGSQHKTLSYEEAVSLAVDFYNQPGIDHAFRLRLRA DPQPAWDMTSKPRQELRFVVRETVCRAQDPPASECDFKDNLVRNCTGLFSTER ESPTVIITCDTVPQGHRV↓RRSGWWNGHKRRRGSGTRRGRFSHIAHGGRKGH ERIA	Chen et al., ASN73762
As-CATH3	MGRWGWVLLVLLATLVAAASASQRKMLTYGEAASFAVDFYNQPGIDHTFQLLCV EPQPVWDTTSKSRQEVRFVICETVCPQASNHASECNLKFNLVRNCTWLFSTEQ KSPTSIITCNTVSPGKHV↓PAKPKPRPGKLSSTLHLAPGSDGKPRCHYP	Chen et al., ASN73763
As-CATH4	MQTCWVILLPLLLGAASTEPLTPGTDPPLTPTYAQALATAVDVYNQPGVDFAF RLLEAESRDDWDASTDPLRQLEFTLKETECVGEDQPLDQCDFKDGGAVLDCTGT FSCSEASLMVLVTCQPAEPLPDRV↓RRGLFKKLRRKIKKGFKKIFKRLPPVGVG VSIPLAGRR	Chen et al., ASN73764
As-CATH5	METCLRLLLLLVGAVATAQAQAQAQTQSQSQAGYEDAVTTAVDIFNQESGLPQ AYRLLEAEPQSEWNPSSQAAQPLKFSVKETVCPAQKGNLQCDFKENGLVKDCS GLFTAGKKPPVTAVKCEDTSQEPELV↓TRRKFWKKVLNGALKIAPFLG	Chen et al., ASN73765
As-CATH6	MKSCWALVLLVGCMASAATAQSQLNFNEAVSLAVDFYNRGLAVNNTFQLLRTAPS GDVSSPFEFRRLNFTIMETTCPVGGQPTQGPCQFKENGLVRACVGGFFSAQQVAP LIVVTCEEAPSEPVRV↓TRWLWLLRGGLKAAGWGIRAHNLNRN	Chen et al., ASN73766
As-CATH7	NPPQDLASQPVPQPLKFSIKETECLVSEKRDISQCPFKDKGLVKDCAGIYSAEKKP PIVTANCEDAGQGPQLV↓KRVNWRKVGRNTALGASYVLSFLG	OL889937
As-CATH8	NPPQDLASQPVPQPLKFSIKETECLVSEKRDISQCPFKDKGLVKDCAGLYAEEKEP PVITAKCEDAGQEPQLV↓KRVNWAKVGRTALKLLPYIFG	OL889938
Cp-CATH3	MGRRGWVLLGLATLVAAALASQRKLLSYGEAASFAVDFYNQPGVDHTFRLLDV EPQPAWDTMAKSCQEVRFVVRETVCPTHKLPAASECDFKDNLVRNCTWLFSTKL KLPASIIITCDTMTPGKDI↓HAKPKPKPGKDERGRPGSGSWIGKGTFFSFPITKK PVG	OL889940
Cp-CATH5	MGTCLRLLLLLVGAVATAGLTPPARAQAQAQAQAQASYETAVATAVDIYNQEPGL AQAYRLLEAEPQDSWNPASQAAQPLKFTVKETTCPAQKGNLQCDFKENGLIKD CSGLFTAGKKPPVTDVKVDASQEPELV↓TRKKWWKKVLKGAIKTALK	OL889941

Cp-CATH7	AFPRTPQDLASQPVQPLRFSIKETTCLVSEKRDVRQCPFKDEGLVKDCTGIYSAE KKPPIVTAVCKDAGQEPELV↓KRVNWRKIGLGASYVMSWL G	OL889942
Cp-CATH10	MGRRGWVLLALATLAAGALGSQHRTLSYEEAVSLAVNFYNQGPIDHAFRLLRA DPQPAWDMTSQPRQELRFVVRETVC PRAQDPPASECDFQDNGLVRNCTGLFSTER ESPTVIITCDTATPGQHARV↓RRSGWRDRIKRHRGSDSRLGYMTPFSTNINKG	OL889939
Gg-CATH2	MGRRGWVLLGLATLVAVALGSQHKTLSYEEAVSLAVSFYNQGPIDRAFRLRA DPQPAWDMTSKPRQELRFVVRETVC PRAQDPPASECDFKDHGLVRNCTGLFSMER ESPTVIITCDTVTPGQHVRV↓RRSGWWDWIKGRRGSGSRRGRFTHIAHGSGSKGH GNNGNIA	OL889943
Gg-CATH4	MQTCWVLLLLLLPLLGAASDLPDTPGTDLQPMP SYA QALATAVDVYNQSGSVDA AFQVLEAESRDDWDANEDPLRQLGFRLKETEC PVGEDQPLDQCDFKDGGA VL DCT ATFSCSEASLMVLVTCQPAEPPPTRD↓RRGLFKKLRRKIKKAFKKVFKRLPPVG VGVSIPLSGHR	OL889944
Gg-CATH5	SPQNPSSQAAQPLKFSVKETVCPIAQKGNLQQCNFKENGLIKDCSGLFTA AKKPP VTDVKCVDASQEPELV↓TRRKWKKVLNGAIKIAPYILD	OL889945
Gg-CATH6	MKSCWALVVLVGCMAS TAA AQS QLN FNEAVSLAVDFYNRGLAVNNTFQLLR TAPE GDVVSKPFEFRRLNFTIMETTC PVAGQLPSEPCQFKENGLVRACVGFFSAQQVAP LIVVTCEEAPSEPVRV↓TRWIGLV RGGLKLAGWGLR TYLNRNR	OL889946
Gg-CATH7	MQPCLRALLVLGA AVAVAMAVALPAPPAPAPKGYQEALAAAINTYNQESGLPQAY RLLEAEPQPQWDPASQPVQPLKFSIKETTCLVSEKRDVSQCLFKDKGLVKDCTGI YSVEKQPPIVTAVCKDAGQEPELV↓KRVNWRKVGLGASYVMSWL G	OL889947
Gg-CATH9	MGRRGWVLLGLATLVAVALGSQHKTLSYEEAVSLAVSFYNQGPIDRAFRLRA DPQPAWDMTSKPRQELRFVVRETVC PRAQDPPASECDFKDHGLVRNCTGLFSMER ESPTVIITCDTVTPGQHVRV↓RRSGRWDWIKGRRGSGSRRGHYSTIRRGRKGS GR	OL889948

Am: *A. mississippiensis*; As: *A. sinensis*; Cp: *C. porosus*; Gg: *G. gangeticus*

Table S2: Summary of prediction of identified cathelicidin sequences from *A. mississippiensis*, *A. sinensis*, *C. porosus*, and *G. gangeticus*. Previously described alligator cathelicidin sequences Am-CATH4 [1] and As-CATH1-6 [2] were also recovered in the analysis and are included in this table as a reference.

Name	Genome assembly	Strand	Start	Stop	Missing region	References
Am-CATH1	gi_397460297_gb_JH735204	-	83125	93242	No	-
Am-CATH3	gi_397456510_gb_JH738990	-	0	6010	No	-
Am-CATH4	gi_397462851_gb_JH732650	-	60	12217	N-ter	Barksdale et al.
Am-CATH5	gi_397462851_gb_JH732650	-	24092	34308	No	-
Am-CATH6	AKHW03001069	-	5231	15336	No	-
Am-CATH8	AKHW03001069	-	33404	42943	N-ter	-
Am-CATH11	AKHW03000909	+	2068	12185	N-ter	-
As-CATH1	gi_555310491_ref_NW_005843086	-	367921	378020	No	Chen et al.
As-CATH2	gi_555311385_ref_NW_005842192	+	460	10559	No	Chen et al.
As-CATH3	gi_555311385_ref_NW_005842192	+	5263	15383	No	Chen et al.
As-CATH4	gi_555310491_ref_NW_005843086	-	0	6074	No	Chen et al.
As-CATH5	gi_555311385_ref_NW_005842192	+	25222	35432	No	Chen et al.
As-CATH6	gi_555311385_ref_NW_005842192	+	53173	63350	No	Chen et al.
As-CATH7	gi_555311385_ref_NW_005842192	+	12151	22328	N-ter	-
As-CATH8	gi_555311385_ref_NW_005842192	+	16243	26462	N-ter	-
Cp-CATH3	gi_698053534_gb_JRXG01102469	-	0	6985	No	-
Cp-CATH5	gi_698089567_gb_JRXG01066436	+	4753	14996	No	-
Cp-CATH7	gi_698089567_gb_JRXG01066436	+	0	5837	N-ter	-
Cp-CATH10	gi_698084222_gb_JRXG01071781	-	2052	12151	C-ter	-
Gg-CATH2	gi_699340657_gb_JRWT01256782	-	0	2350	No	-
Gg-CATH4	gi_699490068_gb_JRWT01141868	+	6112	13962	No	-
Gg-CATH5	gi_699490071_gb_JRWT01141865	+	0	4273	N-ter	-
Gg-CATH6	gi_699490068_gb_JRWT01141868	+	0	7535	No	-
Gg-CATH7	gi_699518732_gb_JRWT01120362	+	0	7133	No	-
Gg-CATH9	gi_699359619_gb_JRWT01242099	+	7	10103	C-ter	-

-: in references denotes the current study

Table S3: Vertebrate cathelcidins peptides included in the phylogenetic analysis. Scientific and common names for each species, as well as the cathelcidin peptide names and NCBI accession numbers are listed. Previously described alligator cathelcidins and all crocodylian cathelcidins identified in this study are shown in Table S1.

Vertebrate group	Species	Common name	Peptide	Accession
Amphibian	<i>Odorrana livida</i>	Green cascade frog	OI-CATH2	AXR75914
	<i>Bufo gargarizans</i>	Asiatic toad	Bg-CATH	ANV28414
Bird	<i>Gallus gallus</i>	Chicken	Gga-CATH1	NP_001001605
	<i>Phasianus colchicus</i>	Ring-necked pheasant	Pc-CATH3	ACZ45041
	<i>Coturnix japonica</i>	Japanese quail	Cj-CATH2	BAW94547
	<i>Coturnix coturnix</i>	Common quail	Cj-CATH3	ACZ45043
	<i>Columba livia</i>	Rock pigeon	Cl-CATH	XP_005512199
	<i>Anas platyrhynchos</i>	Mallard	Ap-CATH	ALD83753
	<i>Gallus gallus</i>	Chicken	Gga-CATH2	NP_001020001
	<i>Cygnus atratus</i>	Black swan	Ca-CATH	XP_035410280
	<i>Gallus gallus</i>	Chicken	Gga-CATH3	NP_001298106
	<i>Naja atra</i>	Chinese cobra	Na-CRAMP	B6S2X0
Reptile	<i>Bothrops atrox</i>	Barba amarilla	Batroxicidin	U5KJC9
	<i>Hydrophis cyanocinctus</i>	Asian annulated sea snake	Hc-CATH	AKJ54480
	<i>Python bivittatus</i>	Burmese python	Pb-CATH	XP_007443270
	<i>Python bivittatus</i>	Burmese python	Pb-CATH	XP_007442672
	<i>Pelodiscus sinensis</i>	Chinese soft shelled turtle	Ps-CATH2	XP_006114479
	<i>Trimerodytes annularis</i>	Red-bellied annulate keelback	Ta-CATH	QBZ68899
	<i>Chelonia mydas</i>	Green sea turtle	Cm-CATH2	XP_007066511
	<i>Chelonia mydas</i>	Green sea turtle	Cm-CATH	XP_007066509
	<i>Pseudonaja textilis</i>	Tropical rattlesnake	Pt-CATH1	U5KJJ1
	<i>Bungarus fasciatus</i>	Banded crait	Bf-CATH	B6D434
	<i>Python bivittatus</i>	Python	Pb-CATH	XP_007445262
	<i>Pelodiscus sinensis</i>	Chinese soft shelled turtle	Ps-CATH3	AWW22372
	<i>Crocodylus siamensis</i>	Siamese crocodile	Cs-CATH	AYV89837
	<i>Mus musculus</i>	House mouse	Mm-CATH	AAB88303
	<i>Oryctolagus cuniculus</i>	Rabbit	Oc-CATH	NP_001075774

Mammal	<i>Pan paniscus</i>	Bonobo	Pp-CATH	XP_003818474
	<i>Canis lupus familiaris</i>	Dog	Clu-CATH	NP_001003359
	<i>Ovis aries</i>	Sheep	Bactinecin-11	AAB62000
	<i>Equus caballus</i>	Horse	Ec-CATH3	NP_001075399
	<i>Sus scrofa</i>	Pig	Protegrin-4	NP_999028
	<i>Trachypithecus cristatus</i>	Silvery lutung	Tc-CATH	B6S2X2
	<i>Sarcophilus harrisii</i>	Tasmanian devil	Sh-CATH2	XP_012398889
	<i>Homo sapiens</i>	Human	LL-37	NP_004336
	<i>Bos taurus</i>	Cattle	BMAP-27	NP_777257
	<i>Macaca mulatta</i>	Rhesus monkey	Mmul-CATH	NP_001028681
	<i>Trichechus manatus latirostris</i>	Florida manatee	Tm-CATH2	XP_023586559

Table S4: Antimicrobial activity of the crocodylian cathelicidins. The MIC values of the synthetic peptides were determined in a microdilution assay in MHB. The antibiotic vancomycin was used against Gram-positive *S. aureus* and *E. faecium* whereas polymyxin B was employed against the remaining Gram-negative strains.

Bacteria	MIC in μM ($\mu\text{g/mL}$)						
	As-CATH7	As-CATH8	Gg-CATH5	Gg-CATH7	LL-37	Polymyxin B	Vancomycin
<i>E. cloacae</i>	0.5 (1.3)	0.5 (1.2)	0.5 (1.3)	2 (4.6)	n.d.	0.5 (0.6)	n.d.
<i>S. aureus</i>	4 (10.8)	0.5 (1.2)	1 (2.7)	16 (37)	n.d.	n.d.	0.5 (0.7)
<i>K. pneumoniae</i>	1 (2.7)	0.5 (1.2)	0.5 (1.3)	4 (9.2)	n.d.	0.5 (0.6)	n.d.
<i>A. baumannii</i>	0.25 (0.7)	0.25 (0.6)	0.5 (1.3)	1 (2.3)	n.d.	0.5 (0.6)	n.d.
<i>P. aeruginosa</i>	4 (10.8)	1 (2.4)	1 (2.7)	8 (18.5)	n.d.	0.5 (0.6)	n.d.
<i>E. faecium</i>	>64 (>172)	>64 (>156)	>64 (>171)	64 (148)	n.d.	n.d.	>64 (>93)
<i>E. coli</i>	2 (5.4)	1 (2.4)	4 (10.7)	4 (9.2)	8 (36)	0.5 (0.6)	n.d.
<i>S. Typhimurium</i>	2 (5.4)	1 (2.4)	0.5 (1.3)	4 (9.2)	16 (72)	1 (1.2)	n.d.
<i>P. vulgaris</i>	>64 (>172)	4 (9.7)	8 (21)	>64 (>148)	n.d.	>64 (>77)	n.d.

n.d.: not determined

Table S5: Biofilm inhibitory activity of the crocodylian cathelicidins. The MBIC₉₅ values of the synthetic peptides were determined by a microdilution assay using crystal violet to stain the adhered bacterial biomass. MBIC₉₅ was defined as the minimal peptide concentration capable of inhibiting mean biofilm growth by at least 95% compared to the untreated control.

Bacteria	MBIC₉₅ in μM ($\mu\text{g/mL}$)			
	As-CATH7	As-CATH8	Gg-CATH5	Gg-CATH7
<i>E. cloacae</i>	32 (86)	4 (9.7)	4 (10.7)	16 (37)
<i>S. aureus</i>	4 (10.8)	1 (2.4)	1 (2.7)	4 (9.2)
<i>A. baumannii</i>	1 (2.7)	0.5 (1.2)	0.5 (1.3)	1 (2.3)
<i>P. aeruginosa</i>	>64 (>172)	64 (156)	32 (85)	>64 (>148)
<i>E. coli</i>	32 (86)	1 (2.4)	32 (85)	32 (74)
<i>S. Typhimurium</i>	1 (2.7)	1 (2.4)	1 (2.7)	4 (9.2)

Supplementary Figures

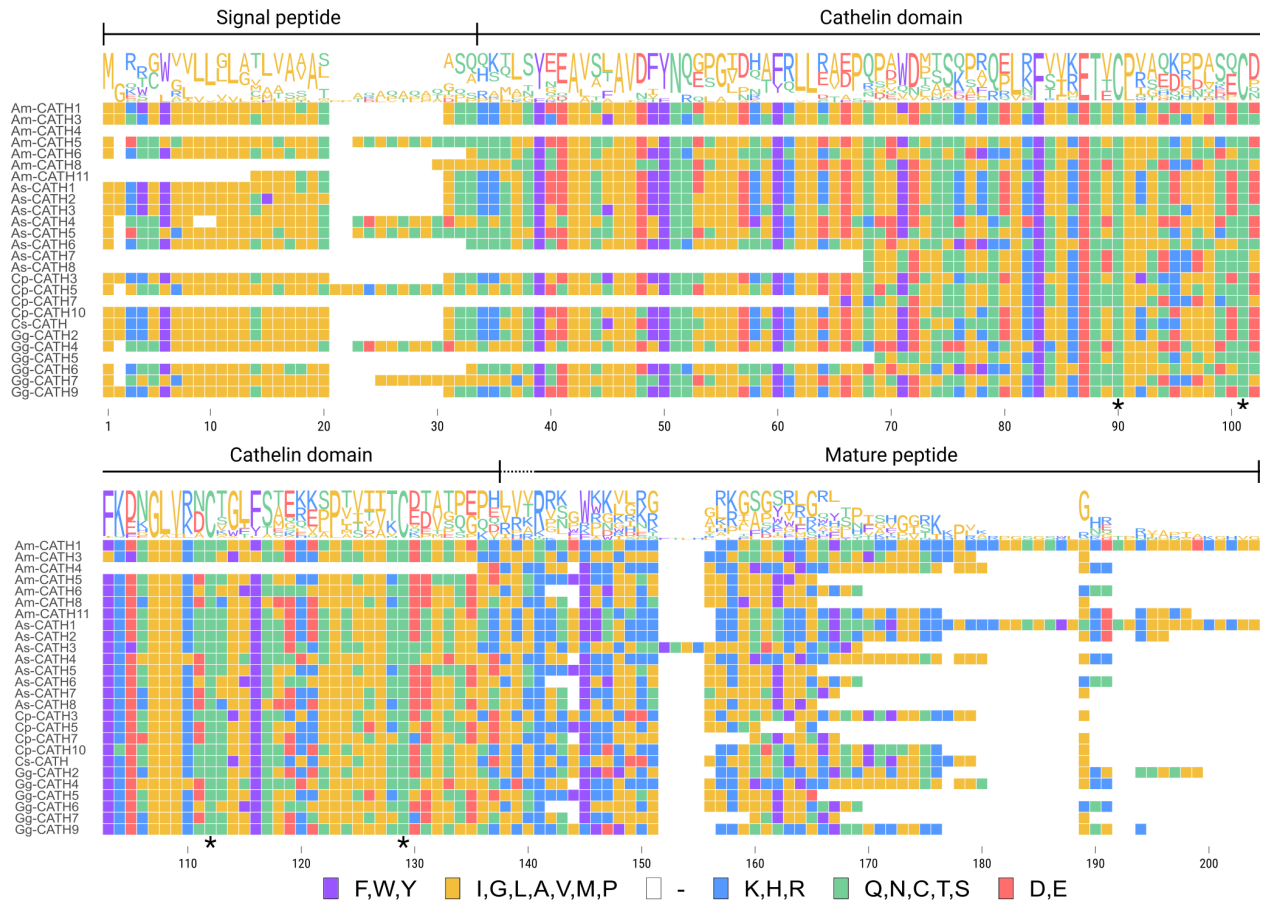


Figure S1: Multiple sequence alignment of novel and previously identified crocodylian cathelicidins. Crocodylian cathelicidins showed the three classical domains present in the cathelicidin family of host defense peptides (HDPs): the signal peptide, cathelin domain, and mature peptide region. The sequences were aligned using the MAFFT algorithm and visualized in R with the package ggmsa version 1.0.3. Amino acid residues are colored according to the Chemistry-AA coloring scheme. Highly conserved cysteines in the cathelin domain are marked with black asterisks (*). Previously described cathelicidins Am-CATH4 [1], As-CATH1-6 [2], and Cs-CATH [3] were also included. Putative elastase cleavage site to process the mature peptide is located within residues 138-140 depending on the sequence. Abbreviations: Am: *A. mississippiensis*; As: *A. sinensis*; Cp: *C. porosus*; Cs: *C. siamensis*; Gg: *G. gangeticus*.

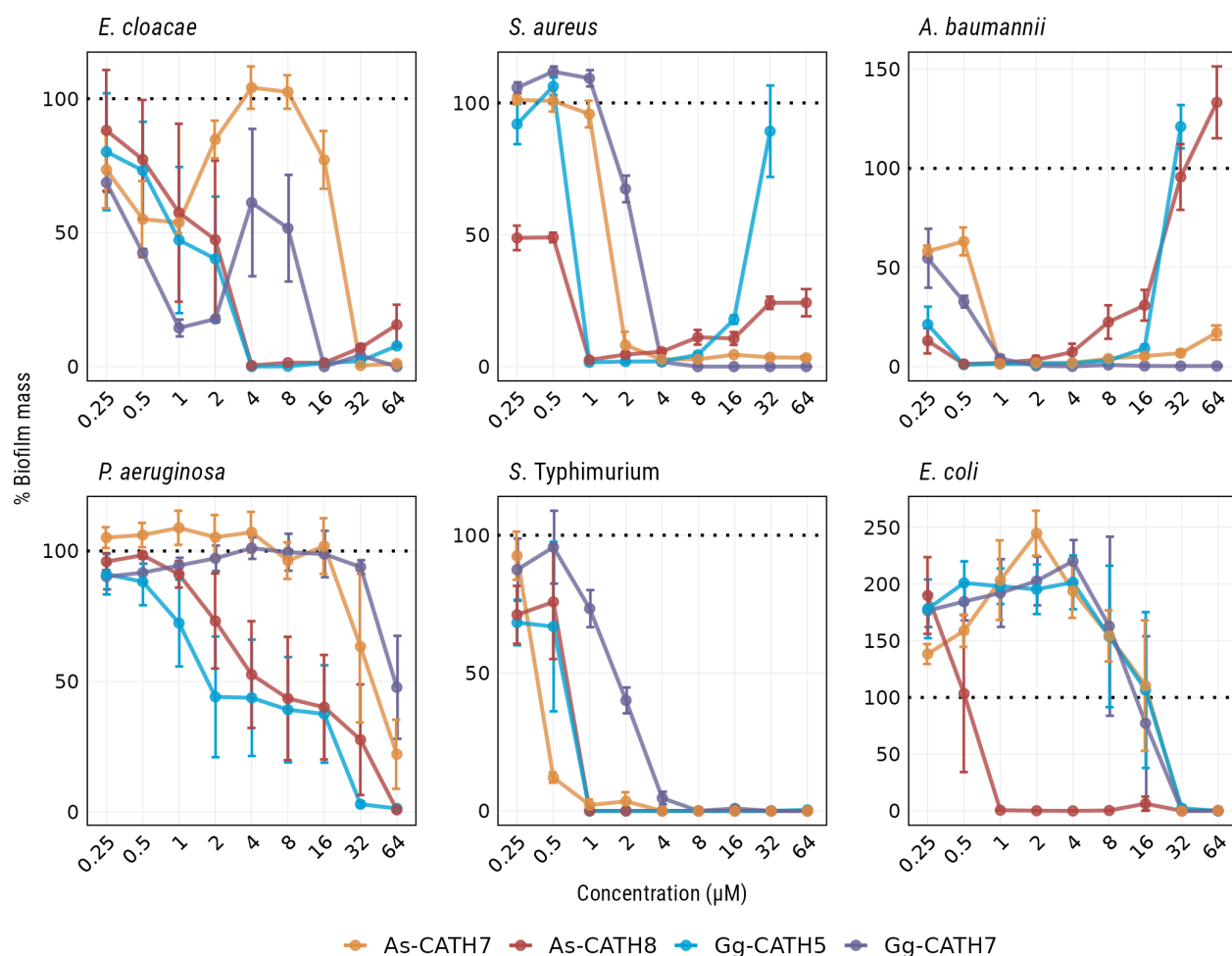


Figure S2: Biofilm inhibitory activity of crocodylian cathelicidin peptides against different bacterial pathogens. Dose-response curves were obtained in different media depending on the bacterial strain and, after 24 h treatment, the adhered biofilm mass was stained with crystal violet. Results are displayed as percentage of biofilm mass with respect to the growth control (defined as 100%). The mean \pm standard error of the mean of at least three biological replicates is shown. Cathelicidins As-CATH8 and Gg-CATH5 enhanced crystal violet staining of *S. aureus* and *A. baumannii* (10% TSB supplemented with 0.1% glucose) at high concentrations. However, this is likely the result of peptide and/or dead bacteria precipitation and not due to an increase in biofilm mass since no bacterial colonies were recovered from these wells. For visualization purposes, the data point corresponding to Gg-CATH5 (64 μ M) is not shown for these two bacteria.

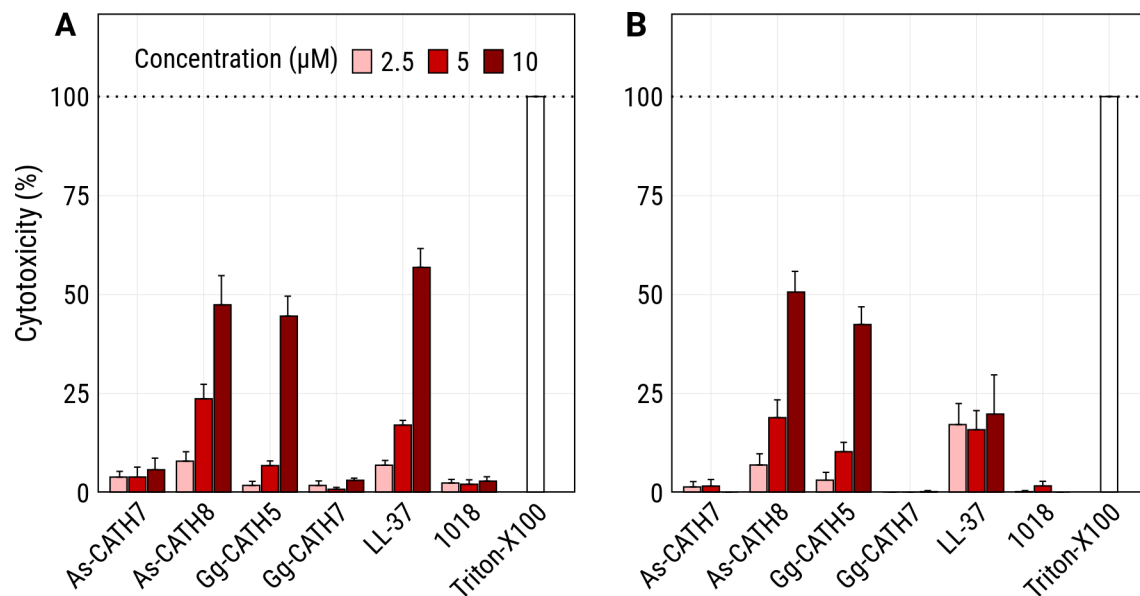


Figure S3: Cytotoxic activity of crocodylian cathelicidins against human cells. The peptide-induced cytotoxicity was measured with the LDH release assay. Values are presented as percentage of cytotoxicity relative to the positive control (cells treated with 2% Triton X-100). Mean \pm standard error of six biological replicates is shown. Human cathelicidin LL-37 and immunomodulatory peptide 1018 were included as a comparison and control, respectively. **A:** Cytotoxicity against the human bronchial epithelial (HBE) cell line. **B:** Cytotoxicity against human peripheral blood mononuclear cells (PBMCs).

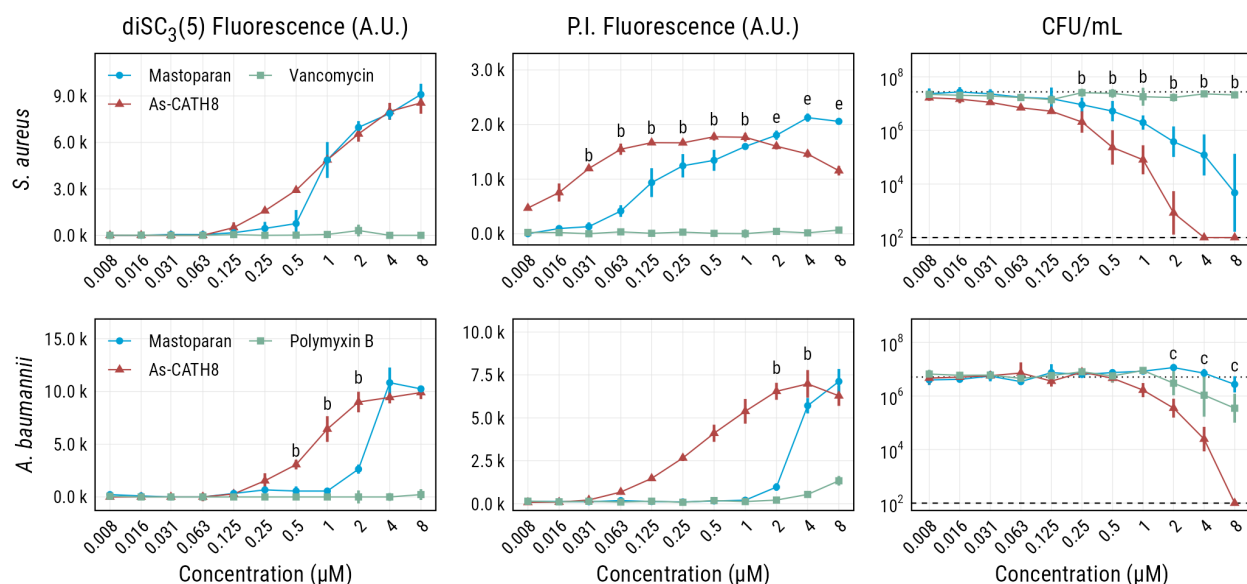


Figure S4: Bacterial membrane depolarization and permeabilization capacity of As-CATH8. The activity against *S. aureus* and *A. baumannii* planktonic cells were evaluated using diSC₃(5) and propidium iodide (PI) dyes, revealing alterations of membrane potential and permeabilization of cells, respectively. The membrane-permeabilizing peptide Mastoparan was used as positive control. Fluorescence readings (arbitrary units), after 1 h treatment against planktonic cells, are shown as mean \pm standard error, whereas CFU data is presented as geometric mean \times / geometric standard deviation. The geometric mean of the CFU counts corresponding to the untreated control is shown as dotted lines. Peptidic antibiotics vancomycin and polymyxin B were used as a comparison for *S. aureus* and *A. baumannii*, respectively. Letters denote statistically significant differences ($p < 0.05$) between As-CATH8 and antibiotics (b), As-CATH8 and Mastoparan (c) or antibiotics and Mastoparan (e), according to the Kruskal-Wallis test followed by the Dunn's post hoc test with the Benjamini-Hochberg correction for multiple comparisons. Experiments were performed at least three times.

Supplementary References

1. Barksdale, S.M.; Hrifko, E.J.; van Hoek, M.L. Cathelicidin Antimicrobial Peptide from *Alligator Mississippiensis* Has Antibacterial Activity Against Multi-Drug Resistant *Acinetobacter Baumannii* and *Klebsiella Pneumoniae*. *Dev. Comp. Immunol.* **2017**, *70*, 135–144, doi:10.1016/j.dci.2017.01.011.
2. Chen, Y.; Cai, S.; Qiao, X.; Wu, M.; Guo, Z.; Wang, R.; Kuang, Y.-Q.; Yu, H.; Wang, Y. As-Cath1-6, Novel Cathelicidins with Potent Antimicrobial and Immunomodulatory Properties from *Alligator Sinensis*, Play Pivotal Roles in Host Antimicrobial Immune Responses. *Biochem. J.* **2017**, *474*, 2861–2885, doi:10.1042/BCJ20170334.
3. Tankrathok, A.; Punpad, A.; Kongchaiyapoom, M.; Sosiangdi, S.; Jangpromma, N.; Daduang, S.; Klaynongsruang, S. Identification of the First *Crocodylus Siamensis* Cathelicidin Gene and Rn15 Peptide Derived from Cathelin Domain Exhibiting Antibacterial Activity. *Biotechnol. Appl. Biochem.* **2019**, *66*, 142–152, doi:10.1002/bab.1709.